

# MADR : METAL ARTIFACT DETECTION AND REDUCTION

Sunil Prasad Jaiswal<sup>a</sup>, Sungsoo Ha<sup>b</sup>, and Klaus Mueller<sup>b</sup>

<sup>a</sup>Multimedia Technology Research Center, Electronics and Computer Engineering, The Hong Kong University of Science and Technology, Hong Kong;

<sup>b</sup>Visual Analytics and Imaging Lab, Computer Science Department, Stony Brook University, New York and SUNY Korea, Incheon, Korea

## ABSTRACT

Metal in CT-imaged objects drastically reduces the quality of these images due to the severe artifacts it can cause. Most metal artifacts reduction (MAR) algorithms consider the metal-affected sinogram portions as the corrupted data and replace them via sophisticated interpolation methods. While these schemes are successful in removing the metal artifacts, they fail to recover some of the edge information. To address these problems, the frequency shift metal artifact reduction algorithm (FSMAR) was recently proposed. It exploits the information hidden in the uncorrected image and combines the high frequency (edge) components of the uncorrected image with the low frequency components of the corrected image. Although this can effectively transfer the edge information of the uncorrected image, it also introduces some unwanted artifacts. The essential problem of these algorithms is that they lack the capability of detecting the artifacts and as a result cannot discriminate between desired and undesired edges. We propose a scheme that does better in these respects. Our Metal Artifact Detection and Reduction (MADR) scheme constructs a weight map which stores whether a pixel in the uncorrected image belongs to an artifact region or a non-artifact region. This weight matrix is optimal in the Linear Minimum Mean Square Sense (LMMSE). Our results demonstrate that MADR outperforms the existing algorithms and ensures that the anatomical structures close to metal implants are better preserved.

**Keywords:** Metal artifacts, CT, detection, anatomical structure.

## 1. INTRODUCTION

Computed X-ray tomography (CT) is a popular technique for medical imaging. However, metals implanted in a patient decrease the benefits of CT imaging since artifacts due to the metals severely reduce the image quality. The problem is that the metal is often near structures of interest, such as pedicle screws in spine surgery, where the artifacts make it difficult to assess the outcome of the procedures. The artifacts are caused by beam hardening, scattering, and noise [1], and they manifest themselves as fine streak artifacts as well as bright and dark band artifacts.

To remove the artifacts, various metal artifact reduction (MAR) algorithms have been proposed [2]. Most of the MAR techniques based on filtered back-projection use sinogram (or projections) interpolations [3-4] as these are computationally very simple. The strategy in these schemes is to detect the parts of the projection data that are affected by metals and then replace the corresponding affected data by data interpolated from sinogram regions adjacent to the corrupted regions [3-5]. Although these algorithms reduce the metal artifacts they fail to recover the exact edge information in the image. They also tend to produce new artifacts and distortions both in the metallic and non-metallic regions. Meyer et al. [6] proposed the frequency shift metal artifact reduction algorithm (FSMAR) that exploits the information hidden in the uncorrected (artifact) image and in the corrected image (obtained by any MAR algorithms). It combines the high frequency components of

---

Further author information: (Send correspondence to Sunil Jaiswal)  
Sunil Jaiswal.: E-mail: spjaiswal@ust.hk, Telephone: +852 9642 4051

the uncorrected image with the low frequency components of the corrected image. While it solves the problems of existing MAR, it introduces new image artifacts because the high frequency of the uncorrected image has both anatomical structures and artifacts, and FSMAR fails to distinguish between them.

Our Metal Artifact Detection and Reduction (MADR) scheme is capable of detecting the artifacts in the uncorrected image and can better control the reduction. It does so by optimally selecting the anatomical structures in the image, discarding the artifacts from the uncorrected image, and produce images with high edge quality (like FSMAR) but also better preserved features. Experimental results demonstrate that the proposed algorithm has superior performance over the existing algorithms in terms of subjective quality.

The remainder of the paper is organized as follows. In Section 2, we present our proposed MADR framework, whereas simulation results are shown in Section 3, and concluding remarks are given in Section 4.

## 2. PROPOSED ALGORITHM

Let the original (artifact free) image and the uncorrected image be denoted as  $\mathbf{F}$  and  $\mathbf{F}_{\text{unc}}$ , respectively. A simple way to reduce the metal artifacts is to apply sinogram based interpolation, as noted above. Let the corrected image by this scheme be denoted as  $F_{MAR1}$ . Then the distortion (denoted as  $D_{MAR1}$ ) between the original  $\mathbf{F}$  component and the interpolated  $F_{MAR1}$  component can be estimated as:

$$D_{MAR1} = F - F_{MAR1}. \quad (1)$$

Let us denote the low frequency component of the uncorrected image  $\mathbf{F}_{\text{unc}}$  and of the interpolated image  $F_{MAR1}$  as  $F_{unc}^L$  and  $F_{MAR1}^L$ , respectively. Similarly, the high frequency components of both of these images are denoted by  $F_{unc}^H$  and  $F_{MAR1}^H$  respectively. FSMAR [6] uses a weighted combination of both the high frequency components, given by:

$$F_{FSMAR} = F_{MAR1}^L + w_1^m \times F_{unc}^H + (1 - w_1^m) \times F_{MAR1}^H. \quad (2)$$

Here  $w_1^m \in [0, 1]$ , is the weighting parameter and is kept high near the metal and zero in the non-metallic regions.

### 2.1 Optimally Designed Weight Matrix

We propose to design the weights such that they can distinguish the artifacts and the anatomical structures in the uncorrected image. With new weights, the proposed metal artifact detection and reduction (MADR) is given by:

$$F_{MADR} = F_{MAR1}^L + w_1 \times F_{unc}^H + w_2 \times F_{MAR1}^H. \quad (3)$$

Here  $w_1 \in [0, 1]$ , is the optimal weighting parameter that controls the contribution of high frequency components of the uncorrected image and  $w_2 = 1 - w_1$ . Substituting  $w_2 = 1 - w_1$  in (3), we can write  $F_{MADR}$  as:

$$F_{MADR} = F_{MAR1}^L + w_1 \times F_{unc}^H + F_{MAR1}^H - w_1 \times F_{MAR1}^H. \quad (4)$$

Replacing  $(F_{MAR1}^L + F_{MAR1}^H)$  by  $F_{MAR1}$  and then rearranging the terms, we get

$$F_{MADR} = F_{MAR1} + w_1 \times (F_{unc}^H - F_{MAR1}^H). \quad (5)$$

Then the distortion (denoted as  $D_{MADR}$ ) between the original  $\mathbf{F}$  component and the proposed  $F_{MADR}$  component can be estimated as:

$$D_{MADR} = F - F_{MADR} = F - F_{MAR1} - w_1 \times (F_{unc}^H - F_{MAR1}^H). \quad (6)$$

Incorporating (1) into (6), and taking squares on both sides, we get

$$\begin{aligned} D_{MADR} &= D_{MAR1} - w_1 A, \\ \implies D_{MADR}^2 &= D_{MAR1}^2 + w_1^2 A^2 - 2w_1(D_{MAR1} \times A). \end{aligned} \quad (7)$$

where  $A = F_{unc}^H - F_{MAR1}^H$ . Then taking the expected value gives,

$$E(D_{MADR}^2) = E(D_{MAR1}^2) + w_1^2 E(A^2) - 2w_1 \times E(D_{MAR1} \times A). \quad (8)$$

Here,  $E(D_{MADR}^2)$  is the mean square error of the proposed algorithm. Our objective is to calculate the weights  $(w_1, w_2)$  such that the distortion in the result image is minimized. To get the optimal weights  $(w_1, w_2)$  in the Linear Minimum Mean Square sense (LMMSE), the problem can be formulated as:

$$\begin{aligned} \min_{w_1, w_2} \quad & E[D_{MADR}^2] \\ \text{s.t} \quad & \sum_{i=1,2} w_i = 1, \quad \text{and} \quad 0 < w_i < 1, \forall i \end{aligned} \quad (9)$$

The above problem has a closed form solution and to get the optimal weights, we differentiate  $E[D_{MADR}^2]$  with respect to  $w_1$ . The optimal weights are

$$\begin{cases} w_1 = E[D_{MAR1}A]/E[A^2] \\ \implies w_1 = E[D_{MAR1} \times (F_{unc}^H - F_{MAR1}^H)]/E[(F_{unc}^H - F_{MAR1}^H)^2], \\ w_2 = 1 - w_1. \end{cases} \quad (10)$$

These optimal weights effectively detect the artifacts occurring in the uncorrected image. To remove these artifacts we substitute (10) in (3) and thus achieve a superior performance. Unfortunately, to estimate  $D_{MAR1}$  in (10) requires an original F which is not available in practice. We propose to use a prior image as an estimate of the original image F.

### 3. SIMULATION RESULT

We implemented the proposed MADR algorithm and compared it with the existing methods. For this purpose, we created a 2D phantom and placed three metal objects of different shape near some small anatomical structures so that the efficiency of the different algorithms could be studied. To obtain the prior we can employ an image from the same or different patients as has been done in [7]. In spine surgery often a pre-op scan is available which can be applied as a prior. For our experiments we generated such a prior by deforming the ground truth image (see Fig. 2(a)).

### 3.1 Visual Analysis of the Weight Map

The contribution of the proposed algorithm is in providing a mechanism that can optimally select the anatomical structures and discards the artifacts. In Fig. 1 we show the weight map used by the FSMAR [6] and the weight map generated by the proposed MADR algorithm. In both of these algorithms, if the weights are close to zero (or small), then the high frequency components of the uncorrected image are not used (see Eq. (2) for FSMAR and Eq. (5) for MADR). Conversely, if the weights are high then the high frequency components of the uncorrected image are utilized. The artifact free phantom (ground truth) is shown in Fig. 1(a) (with a blue box) and the uncorrected image is shown in Fig. 1(b). From Fig. 1(c) it is quite clear that FSMAR only focuses near the metal region whereas MADR (Fig. 1(d)) covers the entire image. In Fig. 1(f) the blue arrow denotes the artifacts whereas the red arrow denotes the circular anatomical structure near the metal. Fig.1 (g) shows the corresponding weight map obtained by FSMAR and we observe that FSMAR fails to distinguish the artifacts and the anatomical structure and thus assigns random weights. Whereas Fig. 1(h) is the weight map of the proposed MADR where we see that it can detect the artifacts and thus assigns small weights in the artifact regions whereas in case of circular anatomical structure (near the metal) it assigns higher weights.

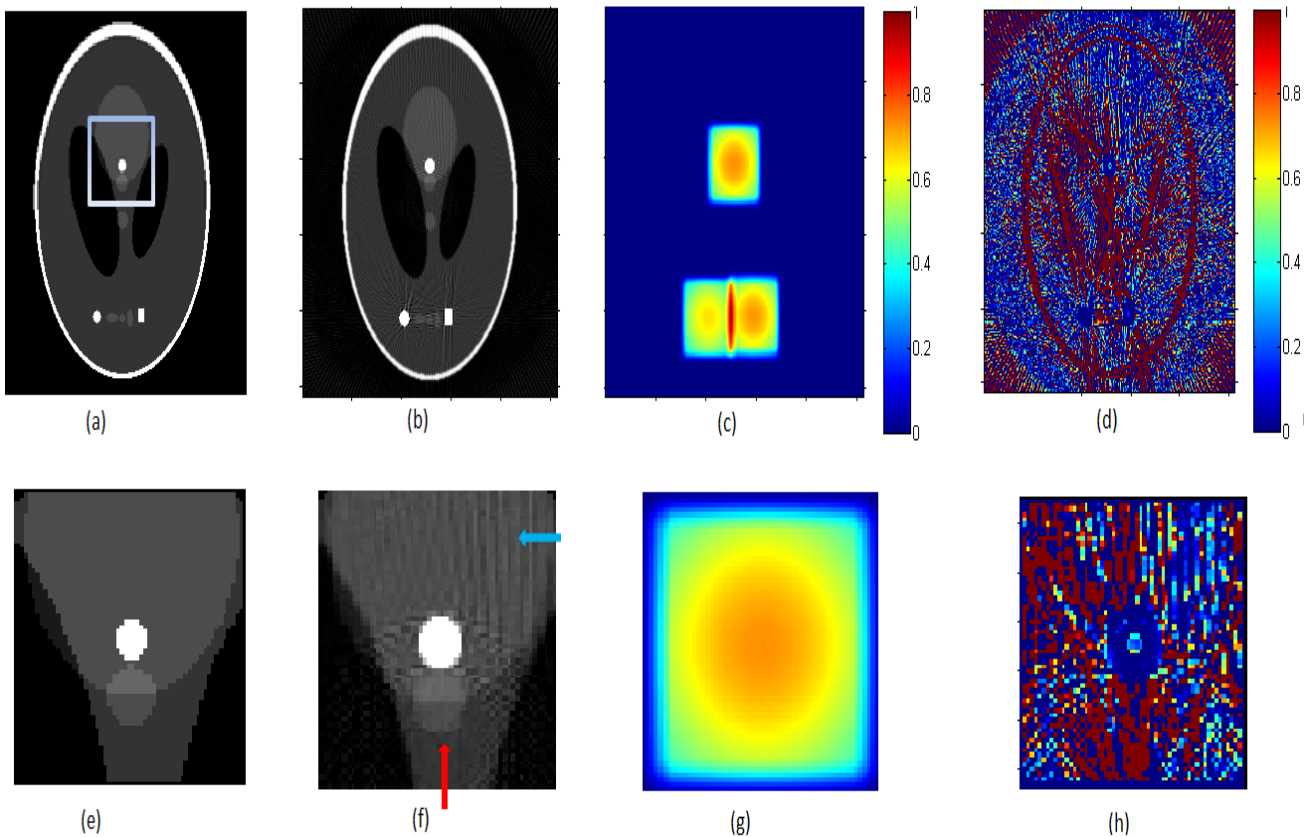


Figure 1. Weight map analysis: (a) Ground Truth Image, (b) Uncorrected Image, (c) FSMAR weight map ( $w_T^m$ ), (d) Proposed weight map ( $w_1$ ) and (e,f,g,h) are the zoomed versions of the blue box shown in (a).

### 3.2 Metal artifact reduction comparison

In Fig. 2, we compare the performance of MAR1 [3] and FSMAR with the proposed MADR. We observe that the streak artifacts are removed successfully by MAR1 (Fig 2(b)) but the anatomical structures near the metal are blurred and there are also other artifacts. FSMAR [6] on the other hand has better image quality (Fig. 2(c)) but some artifacts close to the metal still exist. This is because FSMAR does not differentiate between

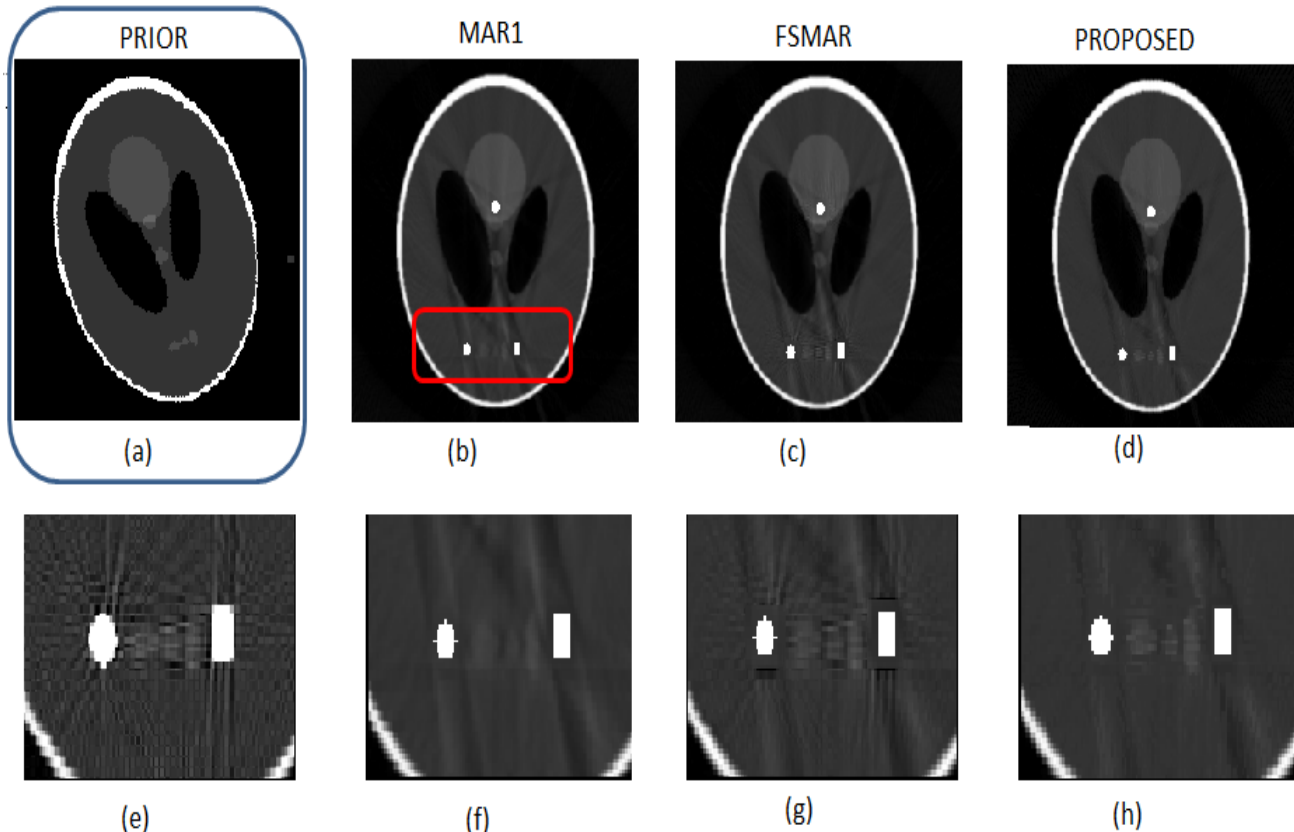


Figure 2. Comparison between different algorithms: (a) Prior Image, (b) Reconstruction by MAR1, (c) FSMAR, (d) Proposed MADR algorithm, (e) Zoomed version of the uncorrected image, (f,g,h) Zoomed version of the corrected image by MAR1, FSMAR and Proposed MADR Algorithm

the artifacts and the anatomical structures. Moreover FSMAR works only near the metal region. Finally, the proposed MADR produces images with considerably less artifacts (Fig. 2(d)) and we observe that the shape of the anatomical structure can be well preserved.

#### 4. CONCLUSION

In this paper, we have proposed a novel method that can differentiate between metal artifacts and true anatomical structure in an uncorrected CT image and then perform the metal artifact reduction accordingly. First experimental results are promising. Its focus on restoring regions near metal objects makes it an attractive scheme for spinal surgery where the regions of interest are typically right next to the inserted metal. The use of more realistic priors will be studied.

#### ACKNOWLEDGMENTS

This research was partially supported by the MSIP (Ministry of Science, ICT and Future Planning), Korea, under the ICT Consilience Creative Program (IITP-2015-R0346-15-1007) supervised by the IITP (Institute for Information and communications Technology Promotion).

## REFERENCES

- [1] Boas, F. E., Fleischmann, D., “CT artifacts: Causes and reduction techniques,” *Imag. Med.*, vol. 4, pp. 229240 (2012).
- [2] Mouton, A., Megherbi, N., Slambrouck, K. V., Nuyts, J., Breckon, T. P., “An experimental survey of metal artefact reduction in computed tomography,” *Journal of Xray Sci Technol.*, 21(2):193-226 (2013).
- [3] Kalender, W. A., Hebel, R., Ebersberger, J., “Reduction of CT artifacts caused by metallic implants,” *Radiology*, vol. 164, no. 2, pp. 576 (1987).
- [4] Abdoli, M., Ay, M. R., Ahmadian, A., Zaidi, H., “A virtual sinogram method to reduce dental metallic implant artefacts in computed tomography-based attenuation correction for pet,” *Nuclear medicine communications*, vol. 31, no. 1, pp. 22 (2010).
- [5] Meyer, E., Raupach, R., Lell, M., Schmidt, B., Kachelrie, M., “Normalized metal artifact reduction (NMAR) in computed tomography,” *Medical Physics*, vol. 37, no. 10, pp. 5482-5493 (2010).
- [6] Meyer, E., Raupach, R., Lell, M., Schmidt, B., Kachelrie, M., “Frequency split metal artifact reduction (FSMAR) in computed tomography,” *Medical physics*, 39(4), 1904-1916 (2012).
- [7] Xu, W., Ha, S., Mueller, K., “Database-assisted low-dose CT image restoration,” *Medical physics*, 40(3):031109 (2013).